Special Section: Frontiers of Hydropedology in Vadose Zone Research

John R. Nimmo*
Lara Mitchell

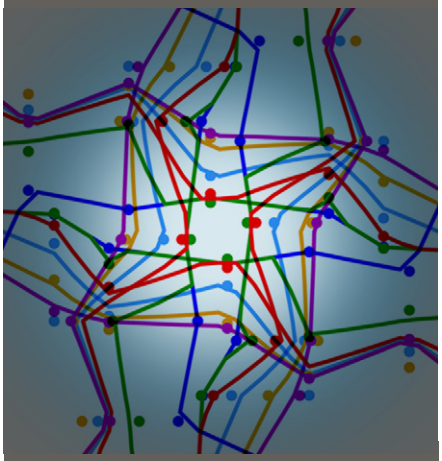

In our two-domain model, a source-responsive domain represents preferential flow. Applied with new elaboration of the nature of preferential-domain water and domain-transfer, the model sometimes shows good quantitative agreement and, in all cases, captures the nonsequential character of irregular wetting patterns.

U.S. Geological Survey, 345 Middlefield Rd., MS-420, Menlo Park, CA 94025. *Corresponding author (jrnimmo@usgs.gov).

Vadose Zone J.
doi:10.2136/vzj2013.03.0054
Received 4 Mar. 2013.

Predicting Vertically Nonsequential Wetting Patterns with a Source-Responsive Model

Water infiltrating into soil of natural structure often causes wetting patterns that do not develop in an orderly sequence. Because traditional unsaturated flow models represent a water advance that proceeds sequentially, they fail to predict irregular development of water distribution. In the source-responsive model, a diffuse domain (D) represents flow within soil matrix material following traditional formulations, and a source-responsive domain (S), characterized in terms of the capacity for preferential flow and its degree of activation, represents preferential flow as it responds to changing water-source conditions. In this paper we assume water undergoing rapid source-responsive transport at any particular time is of negligibly small volume; it becomes sensible at the time and depth where domain transfer occurs. A first-order transfer term represents abstraction from the S to the D domain which renders the water sensible. In tests with lab and field data, for some cases the model shows good quantitative agreement, and in all cases it captures the characteristic patterns of wetting that proceed nonsequentially in the vertical direction. In these tests we determined the values of the essential characterizing functions by inverse modeling. These functions relate directly to observable soil characteristics, rendering them amenable to evaluation and improvement through hydropedologic development.

Abbreviations: REV, representative elementary volume; STVF, surface-tension viscous-flow.

The complex interaction of attributes and processes that control preferential flow in soil is a central challenge of hydropedology (Jarvis et al., 2012). Macropores, fingering, shrinkage/swelling, phase and temperature changes, heterogeneity at all scales, roots, microbiota, fauna, and biofilms are just a few of the factors that collectively cause soil water to flow preferentially through certain pathways while bypassing some fraction of the porous matrix.

A frequently treated aspect of preferential flow is that it can transport water or other substances farther and faster than diffuse flow through the greater body of soil. Effects of high speed or high flux have been the emphasis of a large number of studies (e.g., Thomas and Phillips, 1979; Beven and Germann, 1982; Komor and Emerson, 1994; McCoy et al., 1994; Gish and Kung, 2007; Nimmo, 2007; Nimmo, 2010a).

Besides rapidity of transport, another major consequence of preferential flow is that the patterns of distribution of water and other transported substances can be irregular; as described by Šimůnek et al. (2003), preferential flow "results in irregular wetting of the soil profile as a direct consequence of water moving faster in certain parts of the soil profile than in others." This phenomenon greatly increases the difficulty of prediction and management. Many qualitative studies have been made of irregular wetting patterns, typically by use of dye tracers (e.g., Flury et al., 1994; Kulli et al., 2003; Blume et al., 2009). Quantitative and predictive studies of these irregular patterns are less common.

One-dimensional consideration of preferentially generated irregular patterns renders them more quantitatively approachable. In vertical domain flow dominated by gravity, the irregular patterns can be simply cast as nonsequential flow. In general, instead of a wetting front, we have various depth intervals between the land surface and water table within which water content increases during infiltration, with fastest or earliest wetting not necessarily at the shallowest depths. This nonsequential character has been recognized or highlighted as a preferential flow signature by Graham and Lin (2011), Lin and Zhou (2008), Hardie et al. (2011), and others.

In a traditional treatment of unsaturated flow, surface tension controls the wetted state of individual pores while the principles of noninertial and nonturbulent viscous flow control the movement of water through a network of filled and unfilled pores (Miller and Miller, 1956). Traditionally, these surface-tension viscous-flow (STVF) principles, usually quantified with the Darcy–Buckingham law and Richards' equation, have been used to represent essentially all forms of soil-water flow (Yang et al., 1988). STVF wetting proceeds from wetted parcels of soil to adjacent less-wetted parcels of soil. In other words, the wetted region expands with a wetting front, whether sharp or diffuse. Therefore, this representation is inherently ill-suited to nonsequential flow.

The problem with STVF for nonsequential wetting is not the viscous-flow relations, but rather an overemphasis on surface tension as implemented through capillarity. Capillary relations are used to determine whether a macropore is filled, and being filled is normally equated with flowing. But actual soil-water behavior, including many observations of irregular and fast-developing wetting patterns, suggests that preferential flow commences before macropores are filled.

Many dual-domain approaches to infiltration treat matrix or diffuse flow separately from preferential flow. There is broad consensus that the diffuse-flow domain should be quantifiable using the Darcy–Buckingham law and Richards' equation, but there is no such agreement concerning the best method for the preferential domain. Some alternatives, with varying degrees of reliance on traditional STVF processes, include kinematic waves (e.g., Germann, 1985; Larsbo and Jarvis, 2003), stochastic transfer functions (Jury, 1982), and the water-content-wave formulation of Hincapié and Germann (2009b).

In this paper we elaborate and apply the two-domain source-responsive unsaturated flux model of Nimmo (2010a), referred to as N2010. It is called *source-responsive* because it allows water at depth to sensitively respond to changing conditions at the source of water input. Further explanation and elaboration have been advanced (Nimmo, 2010b; Ebel and Nimmo, 2012; Nimmo, 2012; Cuthbert et al., 2013; Mirus and Nimmo, 2013). Our objective, tested in two case studies, is to predict nonsequential wetting patterns that arise from preferential flow generated by infiltration.

Source-Responsive Model for Infiltration

Basic Flux Model

The N2010 model considers two domains, D for diffuse flow and S for source-responsive flow, corresponding essentially to a relatively fine-pored matrix and interpenetrated macropores, respectively. We use it here as a one-dimensional model extendable in principle to three dimensions. In the D domain STVF principles apply and the Darcy–Buckingham law and Richards' equation quantify the

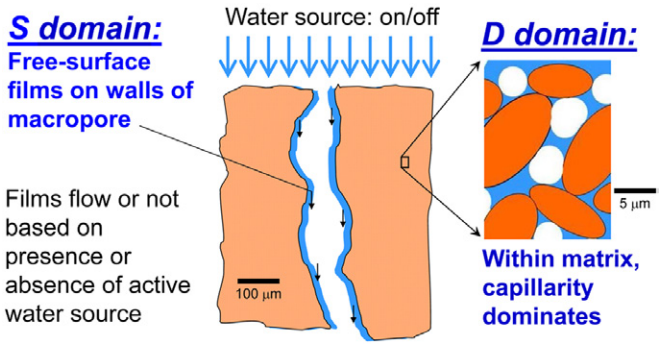

Fig. 1. Source-responsive concepts.

flow. The D domain is characterized by the unsaturated hydraulic conductivity, water retention curve, specific capacity, hydraulic diffusivity, sorptivity, and other traditional soil hydraulic properties of the matrix material. In the S domain flow occurs according to viscous-flow principles but without a major role of surface tension. The S domain is characterized by properties described by Nimmo (2010a), which have potential to be evaluated in a hydropedologic framework, as we discuss below.

Figure 1 shows the S domain in the form of flowing films that cling to macropore walls. Transport rates are relatively high in the direction of flow, allowing a change in conditions at the land surface (e.g., precipitation intensity) to propagate rapidly to various depths in the unsaturated zone. Perpendicular to the direction of film flow, water movement from the film into the matrix tends to be much slower, following traditional STVF principles, and is especially slow in certain cases such as unusually fine pores.

Figure 2 illustrates a mechanism for irregular wetting that this model can account for. A fast flowpath containing little water can quickly make water available at any depth. A volumetric water content (θ) sensor, if sensitive to the internal matrix rather than fast-flowing water in the macropore, would register faster wetting in the layer where abstraction is faster. In traditional concepts, this could be a layer of material with greater sorptivity than the layers above or below. A means of rapid transport of water to depths where it has the opportunity, though not necessity, of being absorbed into the soil matrix is an essential feature of the system.

The S domain includes hydropedologically important features such as wormholes, rootholes, fractures, and interaggregate spaces, wherever the internal walls of a gap within the matrix can support significant flow of a liquid phase. Flow is considered in the form of thick films (a few μm to 10s of μm) on the internal facial area of macropores. Conceptualizing preferential flow as occurring in flowing films makes it easy to formulate flow relations because of the known geometry. In some cases the preferentially flowing water might more closely resemble drops, rivulets, or other forms (Su et

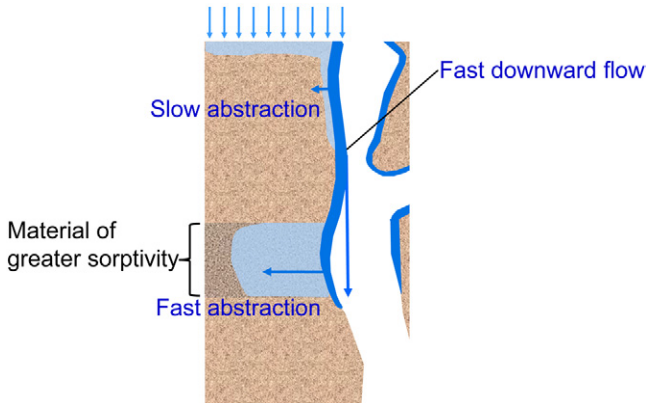

Fig. 2. A hypothetical mechanism for irregular patterns of wetting.

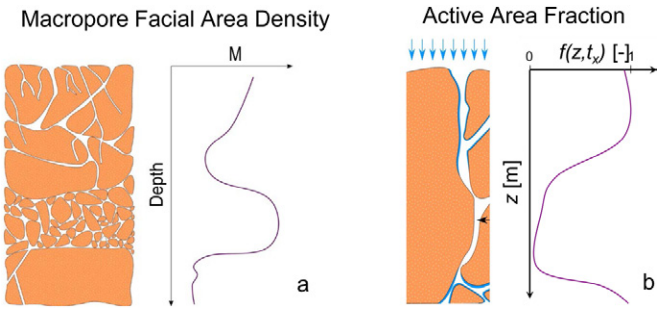

Fig. 3. (a) Example of macropore facial area M as a function of depth. (b) Example of active area fraction *f* as a function of depth at a particular time.

al., 1999). Similarly to the way the grossly irregular geometry of soil pores can be usefully treated as if it were a set of capillary tubes of certain radii, so the irregular geometry of air–water interfaces in unsaturated macropores can be usefully treated as if they were surfaces of films of certain thickness. The key feature for source-responsive flow is that flowing liquid incompletely fills the space within the macropore and therefore is not fully constrained by capillary forces and solid walls. The flow conditions are little-affected by air-water pressure differences but are sensitive to whether or not the macropore is supplied with flowing water. Other consequences include that effective macropore aperture has little influence on either flow capacity or speed, and there is no significant effect of buoyancy to inhibit gravitational flow.

A crucial quantitative characterization of the S domain is the capacity for preferential flow. In the N2010 model, this is the amount of activatable macropore internal facial area per unit volume of the bulk medium [L^{-1}], symbolized M (Fig. 3a). *Activatable* for this purpose means that the area is capable of supporting a flowing water film. This quantity, analogous to the property Hoogmoed and Bouma (1980) defined and termed the contact area, is closely related to fracture frequency indexes used in various fields of earth science, and is geometrically equivalent to the contact length per unit cross-sectional area parameter of Germann and Hensel (2006).

M represents the preferential flow capacity of the medium as a blend of pedologic and hydrologic characteristics. The interfacial area that M represents does not in general equal the total geometric internal wall area of large pores. One reason is that properties of the wall surface area itself may differ from those of the bulk matrix (e.g., Köhne et al., 2002). Hydrophobic portions, for example, would be excluded if they cannot support a flowing film. Additionally, the relevant macropores themselves are distinguished from other pores not fundamentally by size but by hydraulic characteristics. Large pores with insufficient connectivity to a source of input water or to a subsurface region that can accept preferential flow are excluded. These may in effect be dead-end pores that can fill completely when water is copiously available but cannot transmit the water elsewhere except through much smaller pores. Conversely, given that flowing films may be only a few μm thick, smaller pores than what are normally considered macropores may constitute part of the S domain and contribute to M. Thus our use here of the traditional term macropore does not denote the traditional qualifying distinction of pore size.

Another important characterization of the S domain is the proportion of preferential flow capacity that is actively conducting preferential flow at given time. We represent this with an active-area fraction $f(z,t)$, which takes a value between 0 and 1 to indicate the proportion of activatable macropore internal facial area that at a given time is active for conveyance of preferential flow (Fig. 3b). It fluctuates with variations in the source of water and other features of the flow system, and propagates to represent the progress of S-domain flow through the medium. In general f is greater for greater input rates.

The S domain is conceptualized as a set of flowpaths associated with macropores that interact with REVs of the D domain (Fig. 4). Considering an REV of volume δV, the activatable facial area within it is $M\delta V$, and the area activated at a given time is $fM\delta V$. The portion of S-domain water passing through an REV that is not transferred to the D-domain (e.g., if the S flux is large and the activated area $fM\delta V$ is small) goes through and on to other REVs. At the activated area, water can move between domains.

New and Extended Features

For the infiltration-response problem, we developed new features of the N2010 model, chiefly concerning (i) insensibility of water in the S domain, (ii) explicit treatment of domain exchange through a first-order transfer term, and (iii) means of evaluating the properties needed for the source-responsive model. The property-evaluation is performed first in terms of simple parameterizations suitable for inverse modeling, and later in hydropedologic terms.

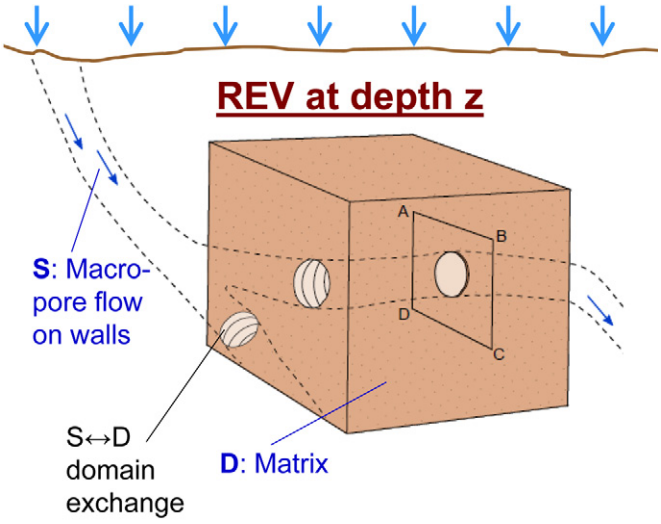

Fig. 4. Idealization of the D and S domains and their response to infiltration.

Because it is normally of very small volume and effectively in a transitional state, water in the S domain is considered to be insensible. D-domain water content is taken as the value that would be measured by an instrument whose region of sensitivity is the REV. S-domain water becomes sensible when it transfers into the D domain. This leaves only one water content θ to be specified for the two-domain model, so it represents both matrix water and total water. The discussion section below explores reasons, evidence, and advantages associated with the effective insensibility of S-domain water.

The interface between S and D domains is the activated internal faces of S-flowpaths (Fig. 4). When conditions permit, S-domain water is absorbed through the activated area into the D domain. Water can also seep out of the matrix into the S-flowpaths if the matrix becomes wet enough (Su et al., 2003). We assume that at a particular water content θ_e, the two domains are at equilibrium so that there is no net flow between them.

For domain exchange as a first-order diffusive process, at a point within the D domain the abstractive flux density is

$$q_{\text{abs}} = -\text{D}(\theta)\frac{\partial\theta}{\partial u} \quad [1]$$

where D is the effective hydraulic diffusivity of the matrix material, and u is a coordinate normal to the S–D interface, positive in the direction into the D domain. A modified formula could include a skin effect, if the medium has a biofilm or other coating that influences the rate of exchange (e.g., Gerke and Köhne, 2002).

Formulation of the transfer rate in terms of water content gradient and diffusivity rather than the more direct matric potential (ψ) gradient and hydraulic conductivity (K) has the advantage that there is no need to introduce matric potential into the problem either for S-domain flow or domain transfer. Additionally, D in general has less water content sensitivity than K, which helps to support an assumption of negligible variation with θ. In a soil experiencing infiltration, near activated portions of macropore walls, the matrix is likely to be in a high water content range with little D variation with θ. In the remainder of this paper we use the assumption that a single value of D is suitable for abstraction processes. Of course the realism of the formulation for first-order transfer is reduced by use of the D–θ form rather than the K–ψ form, because the Darcian flow of water is driven by ψ gradients; the substitution of θ gradients is an artificiality made possible by a functional relation between ψ and θ. Among other shortcomings, it rules out a treatment of θ–ψ hysteresis. The simplification entailed in the D–θ form, however, is in line with other major simplifications of reality made in using this or any other model of unsaturated flow.

We implement the first-order formula Eq. [1] for the abstraction process with consideration of the average distance traversed by a particle of water from the S-active area to the point within the matrix where it ends up as a result of the abstraction. For a simple hypothetical geometry, we consider a cubical REV of volume δV, with all macropores in the form of equally spaced parallel planar fractures. These planar gaps separate the REV into a stack of flat slabs. Assuming a negligible macropore aperture, the slab spacing also equals the slab width, which is the cube width $\delta V^{1/3}$ divided by the number of slabs n. Each slab has two macropore faces of area $\delta V^{2/3}$ so the total facial area $\text{M}\delta V$ must also equal $2\text{n}\delta V^{2/3}$. Equivalently, n equals $\text{M}\delta V^{1/3}/2$, and the slab width is 2/M. On average, a particle of water moving from the face into the slab would have to travel a distance of one-fourth of the slab width or 1/(2M).

The boundary condition at the domain interface is taken to equal θ_e where activated and to equal θ (as within the matrix) otherwise. Then, the difference in water content from the face to the interior of the matrix being θ_e–θ during abstraction, the gradient in Eq. [1] can be approximated

$$\frac{\partial\theta}{\partial u} \approx 2\text{M}[\theta - \theta_e] \quad [2]$$

so that at an activated point on the S–D interface

$$q_{\text{abs}} \approx -2\text{MD}[\theta - \theta_e] \quad [3]$$

The total abstractive flux [$\text{M}^3\,\text{T}^{-1}$] into the REV is this flux density times the activated facial area $f\text{M}\delta V$

$$Q_{\text{absREV}} \approx 2f\text{M}^2\text{D}[\theta_e - \theta]\delta V \quad [4]$$

The rate of change of water content is this flux into the REV divided by the REV volume δV:

$$\frac{\partial \theta}{\partial t} \approx 2 f \mathrm{M}^2 \mathrm{D}\left[\theta_\mathrm{e} - \theta\right] \qquad [5]$$

The numerical coefficient 2 in Eq. [5] serves to account for the specifically planar geometry assumed for the macropores within the REV. More generally the rate of change is

$$\frac{\partial \theta}{\partial t} = \frac{f \mathrm{M}^2 \mathrm{D}}{G}\left[\theta_\mathrm{e}(z) - \theta(z,t)\right] \qquad [6]$$

where G is a dimensionless factor representing the effect of the geometrical configuration of macropores, analogous to the role of the geometric coefficient β of Gerke and van Genuchten (1993).

For the case of nonnegligible flow within the D domain, Eq. [6] can be combined with Richards' equation, giving a formula analogous to Eq. [20] of Nimmo (2010a):

$$\frac{\partial \theta}{\partial t} = \frac{f \mathrm{M}^2 \mathrm{D}}{G}\left[\theta_\mathrm{e}(z) - \theta(z,t)\right] + K(\theta)\frac{\partial^2 \Phi}{\partial z^2} + \frac{\partial K(\theta)}{\partial z}\frac{\partial \Phi}{\partial z} \qquad [7]$$

where Φ is the total hydraulic potential based on gravitational and interfacial forces. From this equation the gravity term at the far right could be omitted for cases where D-domain gravity-driven flow is negligible. Doing so and rewriting the remaining Richards term in the D–θ form yields a simplified expression without K or Φ:

$$\frac{\partial \theta}{\partial t} = \frac{f \mathrm{M}^2 \mathrm{D}}{G}\left[\theta_\mathrm{e}(z) - \theta(z,t)\right] + \frac{\partial \mathrm{D}(\theta)}{\partial z}\frac{\partial \theta}{\partial z} \qquad [8]$$

In this case the gravity acts on water flow exclusively (and implicitly) in the S domain. Beyond the applicability of Eq. [6], Eq. [8] would be useful in the more general case where, in addition to preferential flow, soil water redistributes in response to D-domain moisture gradients. Equation [7] would be useful for the most general case of preferential flow plus moisture gradients and gravity acting in the D domain.

Response to Infiltration

The total infiltration flux density $i(t)$ represents infiltration defined as water moving from outside to inside the system, that is, crossing the soil–atmosphere interface into the soil. We consider infiltration as two components entering the two domains at the land surface:

$$i(t) = i_\mathrm{S}(t) + i_\mathrm{D}(t) \qquad [9]$$

The behavior of water entering the soil as the i_D component, being within the D domain, can be predicted using regular STVF formulas. If it later moves into the S domain, this would be treated as a process of negative abstraction using the domain-exchange formula Eq. [1].

The downward source-responsive flux through the profile can be formulated by applying the continuity equation to Eq. [6], giving

$$\frac{\partial q_S}{\partial z} = -\frac{\partial \theta}{\partial t} = -\frac{f \mathrm{M}^2 \mathrm{D}}{G}\left[\theta_\mathrm{e} - \theta\right] \qquad [10]$$

Integrating and applying the land-surface boundary condition $q_\mathrm{S} = i_\mathrm{S}$ gives the downward source-responsive flux density

$$q_\mathrm{S}(z,t) = i_\mathrm{S} - \int_0^z \frac{f \mathrm{M}^2 \mathrm{D}}{G}\left[\theta_\mathrm{e} - \theta\right] \mathrm{d}z \qquad [11]$$

This formula is analogous to the Darcy–Buckingham law, with which it can be additively combined to represent the total flux density in both domains.

Hydraulic Characterizations

For a simple parameterization, we assume a single M value can represent a finite depth interval. Layers of homogeneous M could be taken as soil horizons or as artificially delineated layers corresponding to instrument placement.

One simple realization of the S-flowpath is a conduit along which water available for S-domain flow moves at uniform speed. From land surface to arrival at depth z, the path has an activation lag time $t_\mathrm{l}(z)$, essentially a characteristic travel time. At time $t_\mathrm{l}(z)$, soil at depth z becomes available for input from the S domain. The degree of activation (f) of source-responsive transport is related to the S infiltration rate. A simple relation for this is

$$f(z,t) = \frac{i_S\left(t - t_\mathrm{l}\right)}{i_0} \qquad [12]$$

The quantity i_0 is the maximum rate of source-responsive infiltration that can occur at the given location. It can be related or equated to the infiltration capacity of the medium or assigned a value based on empirical observations, for example, 30 mm/h as used by Nimmo (2007). Considering dispersion along the path, or source-responsive input at less than the maximum rate, the value determined by the above formula Eq. [12] could be taken to indicate an upper limit.

In the tests in this paper, infiltration goes instantly from 0 to a steady finite value. For this, f at a given depth can be a step function

that goes 0 to 1 at time t_l after start of infiltration. Before the activation time, $f = 0$ and there is no domain transfer.

For values of i_s different from that used in calibration, in principle M(z) does not change but $t_l(z)$ does. We can scale t_l in a simple way using the assumption that the amount of infiltrated water needed to activate a flowpath at given z is the same for different infiltration rates. To derive a scaling formula for this purpose, consider laminar flow of a falling film (Bird et al. (2002), Sec. 2.2) in one S-flowpath. Suppose that the S-path extends downward at an angle α relative to the vertical. Then the average speed of the film in the S-path is

$$V_S = \frac{gL^2 \cos\alpha}{3\nu} \quad [13]$$

where L is the thickness of the film. The volumetric flux through the S-flowpath, by geometric evaluation and using the falling-film formula, is

$$Q = V_S WL = \frac{g\cos\alpha}{3\nu} WL^3 \quad [14]$$

where W is the width of the film. Assuming each S-flowpath always takes the same fraction of i_s, and using the $V_S(L)$ relation,

$$i_S \propto Q \propto L^3 \propto V_S^{3/2} \quad [15]$$

and

$$V_S \propto i_S^{2/3} \quad [16]$$

Because t_l goes as the reciprocal of V_S,

$$t_l \propto i_S^{-2/3} \quad [17]$$

So for predictions where i_S differs from the value used in calibration, this proportionality can scale $t_l(z)$.

Model Testing

Implementation and Solution

During substantial constant-rate infiltration, we assume vertical fluxes are dominated by the S component, and that the D component is negligible. The source-responsive component of Eq. [7] dominates over the two Richards terms, so the much simpler model of Eq. [6] can be solved for water content as a function of time and depth. Assuming constant diffusivity, the solution can be written

$$\theta(z,t) = \theta_e(z) - \exp\left[-\frac{M^2 D}{G}\int f(z,t)\,dt\right] \quad [18]$$

For the step function $f(z,t)$ with activation time $t_l(z)$, we take i_S to be the constant infiltration rate, and i_o to be the maximum rate of source-responsive infiltration described in connection with Eq. [12]:

$$f(z,t) = \begin{cases} 0 & ,t < t_l(z) \\ \dfrac{i_S}{i_o} & ,t \geq t_l(z) \end{cases} \quad [19]$$

The solution Eq. [18] then becomes

$$\theta(z,t) = \begin{cases} \theta_o(z) & ,t < t_l(z) \\ \theta_e(z) - [\theta_e(z) - \theta_o(z)]\exp\left\{-\dfrac{[M(z)]^2 D}{G}\left(\dfrac{i_S}{i_o}\right)[t - t_l(z)]\right\} & ,t \geq t_l(z) \end{cases} \quad [20]$$

where $\theta_o(z)$ indicates initial water content.

Calibration

An appropriate calibration event will have a known or estimable constant infiltration rate and water content measurements with sufficient time and depth resolution to give a clear picture of the water content evolution during infiltration. For measurements made at n discrete depths z_i, i = 1,2,...,n, we work with parameters $\theta_{ei} = \theta_e(z_i)$, $M_i = M(z_i)$, and $t_{li} = t_l(z_i)$. The calibration event is used to find appropriate estimates of θ_{ei}, M_i, and t_{li}, i = 1,2,...,n to describe the water content change in both time and space. The value θ_{ei} is set equal to the observed water content after prolonged infiltration. The remaining parameters M_i and t_{li} are chosen to optimally fit Eq. [20] to the observed water contents. This is most easily done by plotting water content as a function of time separately for each depth. In the case studies here, we have manually optimized M_i and t_{li}, but rigorous optimization methods could be applied. The function M(z) can be fully defined by interpolating between the values M_i, and similarly for the functions $\theta_e(z)$ and $t_l(z)$.

Laboratory Case Study

Measurements of Hincapié and Germann (2009a) for a soil core sample with natural structure provided a suitable test case. The soil, classified as a Cambisol (FAO-UNESCO, 1994) of silt loam texture with an Ah horizon to 0.08 m, B horizon to 0.45 m, and bedrock below 0.45 m, was sampled as a cylinder 0.45 m height and 0.4 m in diameter. Water was applied by sprinkling at different constant input rates while water content was measured by seven TDR probes arrayed vertically. Point symbols in Fig. 5 indicate water content profiles measured during infiltration. Nonsequential wetting patterns are readily apparent. The water content at 0.25 m depth, for example, increases earlier and faster than at 0.18 m depth.

Using the data obtained with an infiltration rate of 20 mm/h (Fig. 5a), we optimized M_i and t_{li} with Eq. [20], obtaining the values in Fig. 6a. Because the infiltration continued long enough that water contents

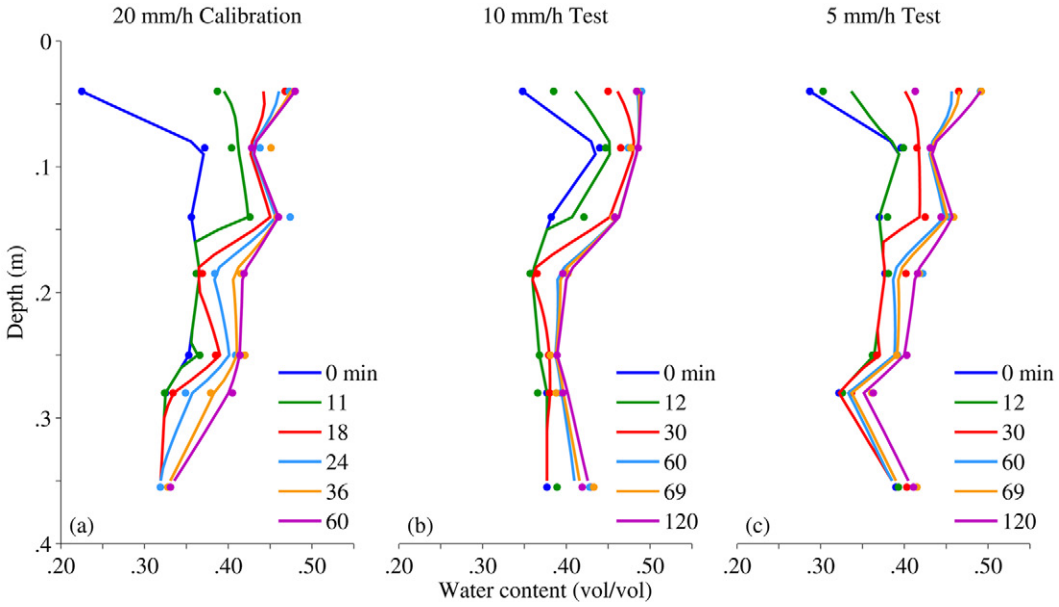

Fig. 5. Measured (symbol) and simulated (line) water contents for the core sample experiments of Hincapié and Germann (2009a). Parameters M(z) and $f(z,t)$ were calibrated with the (a) 20 mm/h infiltration experiment, then used to model the (b) 10 mm/h and (c) 5 mm/h experiments.

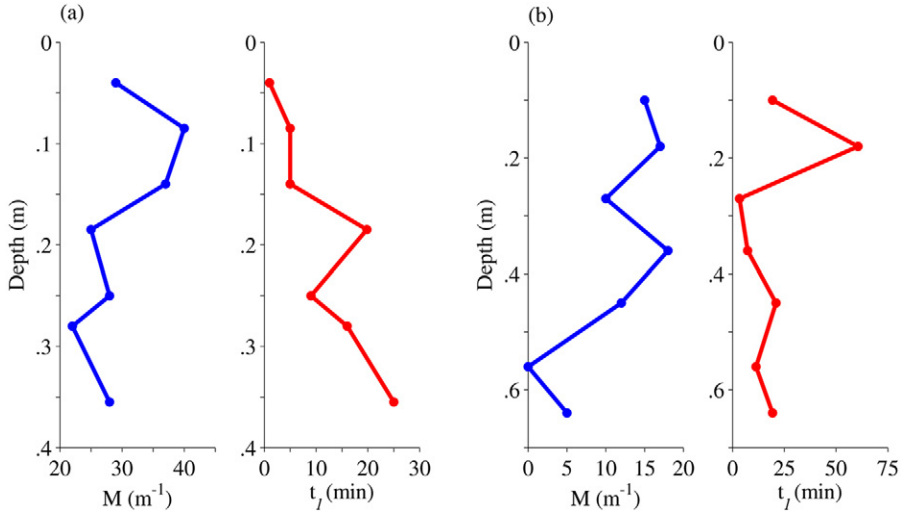

Fig. 6. M(z) and $t_l(z)$ calibrated (a) at the seven depths of TDR sensors for water content data from the 20 mm/h infiltration experiment of Hincapié and Germann (2009a) and (b) at the depths of TDR sensors in the high-infiltration rate, initially dry experiment of Weiler and Naef (2003).

became essentially steady, θ_e values were taken as the maxima when infiltration ceased. Diffusivity was taken as 10^{-2} m^2/h, and G as 0.5.

The connected line segments of Fig. 5 show the predicted $\theta(z,t)$. Using the same 14 parameter values and scaling for the different input rates using Eq. [17], model predictions for the test runs at 10 and 5 mm/h were computed (Fig. 5b and 5c). In the two test cases as well as the calibration case, the predictions, though not precisely hitting all of the measured data, do capture the characteristic behaviors of nonsequential wetting.

The effect of M_i and t_{li} values on the model results is apparent from Fig. 5 and 6. Large M, for example, at 0.09 m depth, makes for a rapid increase of θ. This rapidity results from there being much wetted area for water to be extracted from, as well as smaller intramacropore distances for water to travel within the matrix as it wets. A large t_l value, for example, at 0.18 m depth, makes for slow initiation of the abstraction process and therefore a longer time for θ to begin increasing from its initial value.

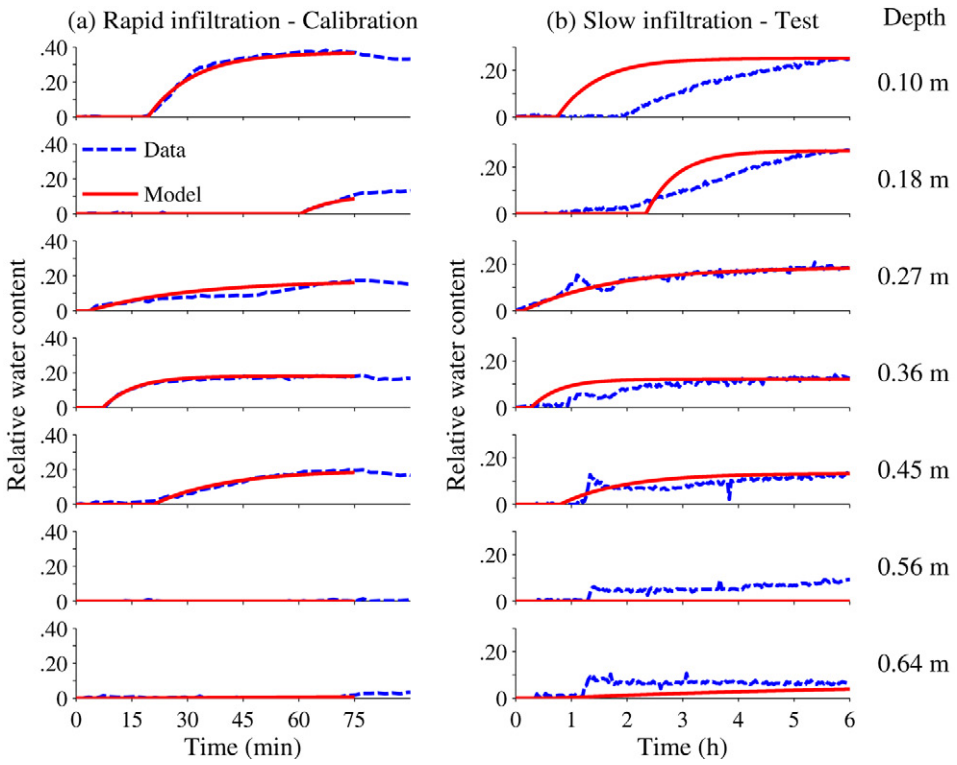

Fig. 7. Measured (dashed) and simulated (solid line) relative water contents for the field experiments of Weiler and Naef (2003), specifically the two experiments that started with low-moisture initial conditions. (a) The high-infiltration-rate calibration case, for which M(z) and $f(z,t)$ were optimized. (b) The low-infiltration-rate case, used to test the model using the calibrated M(z) and $f(z,t)$. Note that the time scales are different; responses are appropriately slower for the low infiltration rate.

Field Case Study

Experiments of Weiler and Naef (2003) in a grassland plot at Rietholzbach, Switzerland, provided field data for a model test. At this and other sites, Weiler and Naef sprinkled instrumented field plots at one of two constant rates, starting from wet or dry initial conditions. The soil at Rietholzbach is a Mollic Cambisol of loam and clay loam texture, with 228 macropores m^{-2} and a macroporosity of 35%. For testing, we selected data obtained with dry initial conditions, for which infiltration had been prevented with a tarp cover for 3 wk before the experiments. In each experiment a total of 75 mm of water was applied. In the high-infiltration-rate case that we used for calibration, this water was applied over 1.1 h, and in the low-infiltration-rate case for testing, over 6 h. Soil water content was measured at 0.1 m depth intervals down to 0.7 m. Weiler (2001) gives further details of the experiments.

Figure 7a shows relative $\theta(t)$ data and model fits at seven depths in the soil profile. Clear differences of behavior at different depths indicate preferential flow. For example, the increase in water content has a substantially delayed start at the 0.18 m depth. Optimizing the model fit to these data produces the M_i and t_{li} parameter values shown in Fig. 6b. The source-responsive model with these values gives a good representation of the magnitude, time behavior, and basic shape of the measured $\theta(t)$. Figure 7b shows how well the model with these parameter values predicts the change in relative water content for the slow-infiltration experiment. As expected, fits are less good than for the calibration case, but the model does predict important gross features of the water response. The relative temporal order of response and approximate magnitude of θ change are predicted reasonably at most of the seven depths. The wetting response at 0.27 m, for example, is correctly predicted to start first, and once started, to change somewhat more gradually than at the two shallower depths. The two deepest depths show a measurable increase of water content for the slow but not the fast infiltration rate, at least over the 1.25 h period in Fig. 7a. Nonpreferential flow modes may be responsible for some of these increases, so a combination of source-responsive and Richards' equation models might better capture the water content changes at the deeper depths. Overall, however, the simpler model reasonably predicts the nonsequential patterns of response apparent in the measurements.

Discussion

Water in Preferential Flow Paths

Postulating that water is insensible while undergoing preferential flow greatly simplifies the mathematical implementation. It permits representation of the effects of preferential flow solely in terms

of the abstraction process, and it also removes the need for a double accounting system for the apportioning of water between domains.

At one level, this assumption can be justified by empirical observation. Many experiments with subsurface instruments and tracers in diverse media show no evidence of preferential flow at positions that preferential flow must have passed near or through to get to positions where it *is* observed. At another level, hydrologic reasoning also supports it. If the total volume of preferentially flowing films or small rivulets is about 1% or less of the soil bulk volume, it would likely be undetectable by conventional instruments such as TDR or neutron soil-moisture probes. Another analog for this negligibility is a two- or three-dimensional system considered as one-dimensional with water sensed by a vertical string of sensors, so that water in a nonvertical flow path is outside the range of detection.

Given our emphasis on incompletely filled macropores that conduct preferential flow, the question arises as to how to consider pores of large aperture when they are completely filled. In this particular type of two-domain configuration, these are best considered as part of the diffuse flow domain, not the preferential domain. This designation is unusual among preferential flow models, but there are physical reasons and evidence to support it. Such pores in the unsaturated medium are likely to be filled not because they are conducting flow at their effective Poiseuille-flow capacity, but because they lack sufficient connectivity to any but very constrictive flow paths. Thus the water flux through them is controlled not by macropore aperture but by the collective conductance of the set of more constricted pores that allow water to flow out of them. Rosenbom et al. (2008), for example, found in field experiments that transport capacity was considerably greater through incompletely filled wormholes in an unsaturated soil than through water-filled wormholes. Such flow is amenable to STVF interpretation and formulation, so it is most usefully considered as part of the STVF-formulated D domain.

Additional evidence for the thinness of preferential flow paths comes from investigations that have evaluated the effective size spectrum of pores that conduct preferential flow (Kung et al., 2005; Germann and Hensel, 2006; Kung et al., 2006). These have shown the effective pore size to be concentrated within a range of surprisingly small radii. Germann and Hensel estimated effective Poiseuille radii of preferentially conducting pores ranging from 5 to 30 μm. The two Kung et al. studies estimated pore frequency distributions to cover a range of smaller effective pore radius, with peaks less than 2 μm (2005) and less than 5 μm (2006). Traditional macropore radii are expected to be 75 μm or more (Soil Science Glossary Terms Committee, 2008). It is more likely that the inferred sizes of preferential flow conduits indicate small fractions of filled pore space within large pores than fully filled capillary pores of such small radius.

Water in the Soil Matrix

STVF concepts represent the water in the portion of the medium not directly subject to preferential flow, the D domain or soil matrix. The linkage to preferentially transported water is determined by the S-domain characteristics and one D-domain characteristic, the equilibrium water content θ_e. This parameter represents a quantitative discrimination between conditions for net flow from matrix to macropores, or vice versa. As a threshold criterion for direction of domain transfer during infiltration, it could be useful in models related to elucidation of the old-water/new-water mix observed in subsurface stormflow (e.g., Klaus et al., 2013).

The value of θ_e could be taken as a measured field-saturated water content, the water content the soil comes to when exposed to a copious infiltration under natural conditions. Alternatively, from an extensive record of measured $\theta(t)$, θ_e could be designated as a value that is exceeded only during unusually wet events.

Hydropedologic Treatment

Hierarchical, Interconnected Structure

One major way in which the source-responsive model, in particular the M and *f* functions it uses to characterize flow, has a strongly hydropedologic character is that it relates to the soil not in terms of arbitrarily isolatable units, but as a complex body of hierarchical structure. The structure is less analogous to discrete building blocks than to an intertwining of components whose structural character derives significantly from their relationship and interaction with each other. The values of M and *f* at a given position depend on a collective set of features of the body of soil, including pathway connections, sources, and sinks possibly some distance away, and in multiple horizons. This contrasts with a traditional STVF approach, in which properties like hydraulic conductivity and water retention are independently definable for a specific horizon or portion of a horizon, and the behavior of the profile is charted after incorporation of the separate units are combined in a computational framework. The source-responsive approach recognizes that soil-water properties cannot be entirely locally based because at any given subsurface point they may be determined in part by features of remote parts of the soil profile, for example, impeding horizons above or below. The source-responsive model's lack of systematic depth dependence of transport time, essential to its ability to predict nonsequential wetting, recognizes that preferential flow paths can differ in how they pass through and how they interact with different layers of soil. One soil horizon may be characterized by strong continuity of preferential flow paths or minimally sorptive matrix material. Such a horizon would show slow θ response. Another might be characterized by the termination of many preferential flow paths or high matrix sorptivity and because of this would show a stronger and faster response regardless of its position in the soil profile.

Hydropedologic Features

Hydropedologic relationships may lead to fruitful estimation techniques for characterizing preferential flow through the source-responsive model. Jarvis et al. (2012) noted that soil characteristics discerned from evaluation of soil structure-related factors like soil aggregation, biologic influences, and patterns of soil genesis have potential for quantifying characteristics of soil water flow. Such pedologic features, also including clay films, soil structures, root distributions, ped coatings, and hydromorphic features (Lin et al., 2006) are directly related to what gives M its particular value at a position in the soil profile.

Basic soil structural description could be a major source of information to determine the quantitative value of M to represent the soil's capacity for conveying preferential flow. Given a likely dependence on macropore orientation, blocky structure might tend to produce larger M than platy structure, and prismatic structure more than either. Finer peds might give larger M than coarser peds. Structural grade may also have significant influence, likely with stronger aggregation causing greater M. To estimate STVF hydraulic characteristics controlling infiltration, Lepore et al. (2009) developed a model to use such structural characteristics. An analogous development could produce a model that estimates M from available soil structural information. A likely course of such development would be, for different horizons of a number of soils, to determine M by other means such as inverse modeling of water-content distribution and statistically correlate those results with each horizon's structural description.

Pedologic structural descriptions also should be useful for the geometric factor G. The physical interpretation of G is that it is the average distance, expressed dimensionlessly in medium-dependent units of 1/M, traveled by a particle of water that undergoes abstraction from a macropore wall into the matrix material in a process that maintains spatial uniformity of water content in the matrix. The 1/M length scaling means that it is not ped size but shape that needs to be considered. From the starting point of the G value 0.5 for the equal-width slabs described above, if the macropores had finite aperture, making the slab width less than 2/M, G would have a value somewhat smaller than 0.5. If instead the macropores are cylindrical, with the same values of M and macroporosity as for the medium of planar macropores, G would be somewhat greater, to account for the greater average distance that water must travel to keep matrix water content uniform. Conversely, if the macropores were interaggregate spaces between cylindrical aggregates, G would be less. In general, internally concave macropore walls, as for wormholes, cause G to have a greater value, and vice versa if they are convex. Following the reasoning laid out above with respect to M, more rounded peds would likely go with a smaller G value than less rounded ones, and platy peds might go with smaller G values than blocky, columnar, or prismatic ones.

Future Development

Clearly a major need is development of practical means of determining the values of the functions M and f. As discussed above, one of the most promising lines of approach is by relating source-responsive hydraulic properties directly to the relevant pedologic descriptions. These may relate as well or better to the important hydraulic characteristics than the STVF properties of unsaturated hydraulic conductivity and water retention relate to the textural data widely used in their estimation.

For the source-responsive model as a whole, there are many options for further development. One obvious possibility is to solve the combined source-responsive/Richards'-equation formula of Eq. [7]. Early tests using a modification of the VS2DT code (Healy, 2008) have shown this is possible. Another is to incorporate θ dependence of hydraulic diffusivity in the domain-transfer term, especially for use when θ at the depths measured starts increasing from a value substantially less than θ_e. For some applications, it would be worthwhile to develop a systematic variation of flow-controlling properties with time, to accommodate shrinking and swelling, development or degradation of soil structure, and other factors. The model could be extended to three-dimensional flow, which would entail complexities arising from the unidirectionality of gravitational force, but would greatly expand its applicability. Another option would be to add a kinematic wave expression as an alternative to the D-domain gravity term, to further reduce reliance on Richards' equation in the general case.

Conclusions

Our elaboration of the Nimmo (2010a) model of preferential flow to predict soil water response to infiltration is useful for cases where preferential flow causes nonsequential wetting of soil layers at different depths. Compared to other two-domain models dealing with preferential flow, this model is distinctive in that one of the two domains employs source-responsive rather than STVF principles of flow. We have elaborated the N2010 model mainly in the treatment of domain transfer and in terms of the state of water in the preferential domain. The basic model employs the quantitative indicators of preferential flow capacity and of degree of flowpath activation that can be determined from $\theta(z,t)$ data. To represent the abstraction of water from the preferential to the matrix domain, we use a diffusivity-based first-order transfer term. The other main innovation we introduce here is a recognition that the water undergoing rapid source-responsive transport at any particular time is of negligibly small volume; it becomes sensible at the time and depth where domain transfer occurs. Besides making possible the prediction of irregular patterns of wetting, this modification affords a major simplification of the mathematics. A direct analytical solution proved sufficient for the measured results we applied it to.

In two test applications, from laboratory and field studies of infiltration into soil of naturally complex structure, in some cases the model shows good quantitative agreement. In all cases it captures the characteristic patterns of wetting that proceeds irregularly in space and time.

We have so far applied the model with the values of the source-responsive preferential flow-characterizing functions $M(z)$ and $f(z,t)$ determined by inverse modeling using representative portions of available $\theta(z,t)$ data. Because these characterizing functions have direct physical interpretations associated with observable features of a soil profile, there is opportunity and likelihood of improved results through hydropedologic development.

Acknowledgments

We are grateful to Ingrid Hincapié and to Markus Weiler for furnishing tabular data from their experiments and for consultation on experimental conditions. We appreciate insights from many helpful discussions with Rick Healy, Ben Mirus, and Kim Perkins, among others.

References

Beven, K., and P. Germann. 1982. Macropores and water flow in soils. Water Resour. Res. 18:1311–1325. doi:10.1029/WR018i005p01311

Bird, R.B., W.E. Stewart, and E.N. Lightfoot. 2002. Transport phenomena, 2nd ed. John Wiley and Sons, New York.

Blume, T., E. Zehe, and A. Bronstert. 2009. Use of soil moisture dynamics and patterns at different spatio-temporal scales for investigation of subsurface flow processes. Hydrol. Earth Syst. Sci. 13:1215–1234. doi:10.5194/hess-13-1215-2009

Cuthbert, M.O., R. Mackay, and J.R. Nimmo. 2013. Linking soil moisture balance and source-responsive models to estimate diffuse and preferential components of groundwater recharge. Hydrol. Earth Syst. Sci. 17(3):1003–1019 doi:10.5194/hess-17-1003-2013

Ebel, B.A., and J.R. Nimmo. 2012. An alternative process model of preferential contaminant travel times in the unsaturated zone–Application to Rainier Mesa and Shoshone Mountain, Nevada. Environ. Model. and Assess. 18:345–363. doi:10.1007/s10666–012–9349–8

FAO-UNESCO. 1994. Soil map of the world. ISRIC, Wageningen, the Netherlands.

Flury, M., H. Flühler, W.A. Jury, and J. Leuenberger. 1994. Susceptibility of soils to preferential flow of water—A field study. Water Resour. Res. 30(7):1945–1954. doi:10.1029/94WR00871

Gerke, H.H., and J.M. Köhne. 2002. Estimating hydraulic properties of soil aggregate skins from sorptivity and water retention. Soil Sci. Soc. Am. J. 66(1):26–36. doi:10.2136/sssaj2002.0026

Gerke, H.H., and M.T. van Genuchten. 1993. Evaluation of a first-order water transfer term for variably saturated dual-porosity flow models. Water Resour. Res. 29(4):1225–1238. doi:10.1029/92WR02467

Germann, P.F. 1985. Kinematic wave approach to infiltration and drainage into and from soil macropores. Trans. ASAE 28:745–749.

Germann, P.F., and D. Hensel. 2006. Poiseuille flow geometry inferred from velocities of wetting fronts in soils. Vadose Zone J. 5:867–876. doi:10.2136/vzj2005.0080

Gish, T.J., and K.-J.S. Kung. 2007. Procedure for quantifying a solute flux to a shallow perched water table. Geoderma 138(1–2):57–64. doi:10.1016/j.geoderma.2006.10.014

Graham, C.B., and H.S. Lin. 2011. Controls and frequency of preferential flow occurrence: A 175-event analysis. Vadose Zone J. 10:816–831. doi:10.2136/vzj2010.0119

Hardie, M.A., W.E. Cotching, R.B. Doyle, G. Holz, S. Lisson, and K. Mattern. 2011. Effect of antecedent soil moisture on preferential flow in a texture-contrast soil. J. Hydrol. 398(3–4):191–201. doi:10.1016/j.jhydrol.2010.12.008

Healy, R.W. 2008. Simulating water, solute, and heat transport in the subsurface with the VS2DI software package. Vadose Zone J. 7:632–639. doi:10.2136/vzj2007.0075

Hincapié, I., and P.F. Germann. 2009a. Impact of initial and boundary conditions on preferential flow. J. Contam. Hydrol. 104(1–4):67–73. doi:10.1016/j.jconhyd.2008.10.001

Hincapié, I.A., and P.F. Germann. 2009b. Abstraction from infiltrating water content waves during weak viscous flows. Vadose Zone J. 8:891–901. doi:10.2136/vzj2009.0003

Hoogmoed, W.B., and J. Bouma. 1980. A simulation model for predicting infiltration into cracked clay soil. Soil Sci. Soc. Am. J. 44:458–461. doi:10.2136/sssaj1980.03615995004400030003x

Jarvis, N., J. Moeys, J. Koestel, and J.M. Hollis. 2012. Preferential flow in a pedological perspective. In: H. Lin, editor, Hydropedology—Synergistic integration of soil science and hydrology. Academic Press, Waltham, MA. p. 75–120.

Jury, W.A. 1982. Simulation of solute transport using a transfer function model. Water Resour. Res. 18(2):363–368. doi:10.1029/WR018i002p00363

Klaus, J., E. Zehe, M. Elsner, C. Külls, and J.J. McDonnell. 2013. Macropore flow of old water revisited: Experimental insights from a tile-drained hillslope. Hydrol. Earth Syst. Sci. 17:103–118. doi:10.5194/hess-17-103-2013

Köhne, J.M., H.H. Gerke, and S. Köhne. 2002. Effective diffusion coefficients of soil aggregates with surface skins. Soil Sci. Soc. Am. J. 66:1430–1438. doi:10.2136/sssaj2002.1430

Komor, S.C., and D.G. Emerson. 1994. Movements of water, solutes, and stable isotopes in the unsaturated zones of two sand plains in the upper Midwest. Water Resour. Res. 30(2):253–267. doi:10.1029/93WR03099

Kulli, B., M. Gysi, and H. Flühler. 2003. Visualizing soil compaction based on flow pattern analysis. Soil Tillage Res. 70(1):29–40. doi:10.1016/S0167-1987(02)00121-6

Kung, K.-J.S., M. Hanke, C.S. Helling, E.J. Kladivko, T.J. Gish, T.S. Steenhuis, and D.B. Jaynes. 2005. Quantifying pore-size spectrum of macropore-type preferential pathways. Soil Sci. Soc. Am. J. 69(4):1196–1208. doi:10.2136/sssaj2004.0208

Kung, K.-J.S., E.J. Kladivko, C.S. Helling, T.J. Gish, T.S. Steenhuis, and D.B. Jaynes. 2006. Quantifying the pore size spectrum of macropore-type preferential pathways under transient flow. Vadose Zone J. 5(3):978–989. doi:10.2136/vzj2006.0003

Larsbo, M., and N. Jarvis. 2003. MACRO 5.0 A model of water flow and solute transport in macroporous soil—Technical description. Stud. in the Biogeophys. Environ. Emergo 2003(6). Dep. of Soil Sci., Swedish Univ. of Agric. Sci., Uppsala.

Lepore, B.J., C.L.S. Morgan, J.M. Norman, and C.C. Molling. 2009. A mesopore and matrix infiltration model based on soil structure. Geoderma 152(3–4):301–313. doi:10.1016/j.geoderma.2009.06.016

Lin, H., J. Bouma, Y. Pachepsky, A. Western, J. Thompson, R. van Genuchten, H.-J. Vogel, and A. Lilly. 2006. Hydropedology: Synergistic integration of pedology and hydrology. Water Resour. Res. 42(5):W05301. doi:10.1029/2005WR004085

Lin, H., and X. Zhou. 2008. Evidence of subsurface preferential flow using soil hydrologic monitoring in the Shale Hills catchment. Eur. J. Soil Sci. 59:34–49. doi:10.1111/j.1365-2389.2007.00988.x

McCoy, E.L., C.W. Boast, R.C. Stehouver, and E.J. Kladivko. 1994. Macropore hydraulics: Taking a sledgehammer to classical theory. In: R. Lal and B. A. Stewart, editors, Advances in soil science. Lewis Publishers, Boca Raton, FL.

Miller, E.E., and R.D. Miller. 1956. Physical theory for capillary flow phenomena. J. Appl. Phys. 27(4):324–332. doi:10.1063/1.1722370

Mirus, B.B., and J.R. Nimmo. 2013. Balancing practicality and hydrologic realism–A parsimonious approach for simulating rapid groundwater recharge via unsaturated-zone preferential flow. Water Resour. Res. 49(3):1458–1465. doi:10.1002/wrcr.20141.

Nimmo, J.R. 2007. Simple predictions of maximum transport rate in unsaturated soil and rock. Water Resour. Res. 43(5). doi:10.1029/2006WR005372

Nimmo, J.R. 2010a. Theory for source-responsive and free-surface film modeling of unsaturated flow. Vadose Zone J. 9:295–306. doi:10.2136/vzj2009.0085

Nimmo, J.R. 2010b. Response to Germann's comment on "Theory for source-responsive and free-surface film modeling of unsaturated flow." Vadose Zone J. 9:1102–1104. doi:10.2136/vzj2010.0088

Nimmo, J.R. 2012. Response to "Comments on 'Theory for source-responsive and free-surface film modeling of unsaturated flow.'" Vadose Zone J. 11. doi:10.2136/vzj2012.0044

Rosenbom, A.E., V. Ernstsen, H. Flühler, K.H. Jensen, J.C. Refsgaard, and H. Wydler. 2008. Fluorescence imaging applied to tracer distributions in variably saturated fractured clayey till. J. Environ. Qual. 37(2):448–458. doi:10.2134/jeq2007.0145

Šimůnek, J., N.J. Jarvis, M.Th. van Genuchten, and A. Gärdenäs. 2003. Review and comparison of models for describing non-equilibrium and preferential flow and transport in the vadose zone. J. Hydrol. 272(1):14–35. doi:10.1016/S0022-1694(02)00252-4

Soil Science Glossary Terms Committee. 2008. Glossary of soil science terms 2008. SSSA, Madison, WI.

Su, G.W., J.T. Geller, K. Pruess, and F. Wen. 1999. Experimental studies of water seepage and intermittent flow in unsaturated, rough-walled fractures. Water Resour. Res. 35(4):1019–1037. doi:10.1029/1998WR900127

Su, G.W., J.R. Nimmo, and M.I. Dragila. 2003. Effect of isolated fractures on accelerated flow in unsaturated porous rock. Water Resour. Res. 39(12). doi:10.1029/2002WR001691

Thomas, G.W., and R.E. Phillips. 1979. Consequences of water movement in macropores. J. Environ. Qual. 8(2):149–152. doi:10.2134/jeq1979.00472425000800020002x

Weiler, M., and F. Naef. 2003. An experimental tracer study of the role of macropores in infiltration in grassland soils. Hydrol. Processes 17(2):477–493. doi:10.1002/hyp.1136

Weiler, M.H. 2001. Mechanisms controlling macropore flow during infiltration—Dye tracer experiments and simulations, Diss. ETHZ No. 14237, Zürich, Switzerland.

Yang, Y.-W., G. Zografi, and E.E. Miller. 1988. Capillary flow phenomena and wettability in porous media—II. Dynamic flow studies. J. Colloid Interface Sci. 122(1):35–46. doi:10.1016/0021-9797(88)90285-8